Gas exsolution and gas invasion in peat

Towards a comprehensive modelling framework

Zhao, H.F.; Muraro, S.; Jommi, C.

DOI
10.1680/jgele.20.00014

Publication date
2020

Document Version
Accepted author manuscript

Published in
Geotechnique Letters

Title: Gas exsolution and gas invasion in peat: a proposal towards a comprehensive modelling framework

Authors

H. F. Zhao*

S. Muraro**

C. Jommi**,***

Affiliation

*School of Civil Engineering, Sun Yat-Sen University, Guangzhou 510275, China.

**Department of Geoscience and Engineering, Delft University of Technology, Stevinweg 1, 2628 CN, Delft, the Netherlands

***Department of Civil and Environmental Engineering, Politecnico di Milano, piazza Leonardo da Vinci 32, 20133, Milano, Italy

Keywords

constitutive relations; organic soils; partial saturation

Correspondence to

Stefano Muraro, Department of Geoscience and Engineering

Delft University of Technology, Stevinweg 1 / PO-box 5048, 2628 CN Delft / 2600 GA Delft, The Netherlands

e-mail: S.Muraro@tudelft.nl

ABSTRACT

Increasing climatic stresses accelerate the degradation of highly organic soils, like peat, by increasing their drying rate above the water table and their decomposition rate under water. Recent experimental studies provide evidence of the consequences of these processes on the hydro-mechanical properties of peat. However, modelling the experimental evidence in a comprehensive framework remains challenging, especially in the case of anaerobic degradation, which is accompanied by gas generation, exsolution and expansion, into an initially saturated matrix of soil. In this research study, experimental results from undrained isotropic unloading on artificially gas-charged peat samples are combined with data from drying tests on the same peat, in an attempt to develop a unified framework encompassing the two desaturation processes. As a first approximation, simple compression laws depending on the average stress acting on the soil skeleton are used to simulate the experimental results. The comparison between experimental data and model simulations suggests the possibility of modelling gas expansion similar to the gas invasion process occurring on drying. The modelling approach, stemming from unsaturated soil mechanics, is meant to offer a possible framework to include the hydro-mechanical consequences of the effects of degradation of peats in the engineering analysis.

INTRODUCTION

A considerable amount of structures and infrastructures in the northern Europe is built on soft organic soils including peats. In the Netherlands, peat covers about 9% of the area country, mostly in its densely populated western part, and is encountered in the foundation of more than 7000 km flood defences and of the urban areas. Recent heat waves and drought periods rose the attention on the effects of water deficit on the rate of degradation of peats, both above and below the water table. The worst consequence of climatic stresses, CO_2 emission, has been studied intensively, to reduce the environmental impact of increased rate of peat degradation (Page et al., 2002; Van der Werf et al., 2009; Minayeva & Sirin, 2012). However, the geotechnical engineering consequences of drying and degradation received less attention in the past. Drying and shrinkage is of concern for surficial peat layers and climate-sensitive infrastructure, while anoxic degradation contributes significantly to land subsidence. Below the water table, dissolved CH_4 and H_2S saturate the pore fluid as a result of the decomposition of the organic matter, and can be exsolved by temperature increase, water table drop or total stress reduction (Vonk et al., 1994; den Haan & Kruse, 2007). Both these mechanisms, drying and gas exsolution, ultimately contribute to significant land subsidence and reduction in available resistance (Wösten et al., 1997; den Haan & Kruse, 2007; Glaser et al., 2004; Acharya et al., 2015).

Recent experimental studies are providing evidence of the consequences of increasing duration of drought periods on the hydro-mechanical properties of peats (Price, 2003; Peng et al., 2007; Gebhardt et al., 2010; Acharia et al., 2016; Jommi et al., 2019). However, the development of comprehensive geotechnical models reliable enough to be included in assessment tools still lags behind. This is especially true in the case of underwater anaerobic degradation, promoting gas generation, exsolution and expansion into an initially saturated matrix of soil.

In the latter case, reference can be made to the broad category of gas-bearing sediments, where gas is typically produced by decomposition of organic matter (Wheeler, 1988). Few constitutive models for fine grained gassy soils have been reported in the literature (Grozic et al., 2005; Sultan & Garziglia, 2014), which assume that the gas pressure coincides with the pore liquid pressure, with the effects of the gas bubbles accounted for through a compressible pore fluid mixture. Recently, gas-liquid pressure difference was accounted for in a consolidation model for peats by Yang & Liu (2016). The model did not include gas exsolution-dissolution and the gas bubbles were assumed to remain confined within the pore fluid without interaction with the soil skeleton. However, recent experimental results by Acharya et al. (2016) and Jommi et al. (2019) suggest that the amount of

gas exsolution and expansion is ruled by the mutual interaction between the gas phase and the solid skeleton.

Possible modelling approaches come from the research on gas hydrate bearing sediments (GHBS). In the dissociation process, the generated gas pressure cannot be disregarded and a description of the unsaturated state of the soil must be accomplished (Kimoto et al., 2007). Different constitutive models for GHBS have been proposed anchored to the concept of water retention curve (Kimoto et al., 2007; Sanchez & Santamarina, 2010; Dai & Santamarina, 2013; Sánchez et al., 2018). Despite the inherent differences between gas exsolution (gassy soils and GHBS) and gas invasion due to drying (unsaturated soils), numerical results from tube-network models by Jang & Santamarina (2014) showed that the fluids pressure difference - water saturation relationships are surprisingly similar to each other.

In this work, experimental results from gas exsolution in peat are combined with data form drying tests on the same peat. Information on the retention properties from drying tests is used to estimate the difference between gas and liquid pressure for a given amount of gas retained in the peat fabric. Preliminary indications on how to include the effects of exsolved gas in a modelling approach are given, in an attempt to develop a unified framework encompassing the two desaturation processes.

MATERIALS AND METHODS

The experimental study was conducted on sphagnum sedge peat specimens, sampled at - 1.0 to - 2.5 m depth, close to the Markermeer in North Holland. The effects of gas were investigated in the triaxial apparatus on natural and reconstituted peat samples artificially charged with CO_2, triggering gas exsolution by decreasing the total isotropic stress under external undrained conditions. A parallel series of tests were conducted to investigate the behaviour of peat upon drying. Experimental data from the drying test with the HYPROP® device (UMS, 2012) and shrinkage test with the balloon method (Ata-Ur-Rehman & Durnford, 1993) were combined to estimate the amount of air that can be retained in the peat fabric as a function of gas - liquid pressure difference. The main index properties and information on the stress path for each test are reported in Table 1. Loss of ignition tests gave an average organic content of 85,7 % (D2974-14, 2014; Skempton & Petley, 1970). Full details on the experimental procedures for the triaxial tests and the drying tests are reported by Jommi et al. (2019) and Trivellato (2014), respectively.

Table 1. Main index properties and information on the stress path for each test

Sample ID	Test	Sample type	Specific density G_s (-)	Initial water content w_i (-)	Initial void ratio e_i (-)	Mean total stress p (unloading) (kPa)	Pressure difference $u_g - u_l$ (drying) (kPa)
SP_NG	Gas	Natural	1.43	6.53*	10.78	409 → 65	
SP_RG	Gas	Reconstituted	1.44	7.88	11.34	406 → 40	
SP_RD	Drying	Reconstituted	1.44	9.10	13.16		0 → 80

* Sample SP_NG was first saturated under back pressure of 405 kPa before being flushed with carbonated water (Jommi et al. 2019)

EXPERIMENTAL RESULTS

Undrained unloading

Gas-bearing soils experience volumetric strains upon undrained unloading as a result of gas exsolution and expansion. Fig. 1 displays the volumetric strain, ε_p, for the gassy samples during isotropic undrained unloading as a function of the applied mean total stress, p. After an initial part of the unloading stage where the pore fluid was under-saturated of carbon dioxide, gas exsolution started. The rate of gas exsolution increased exponentially over unloading. At the end of the test, the gas content attained a volumetric fraction of about 15% of the initial sample volume, in line with some field observation (Landva & Pheeney, 1980; Hobbs, 1986; Reynolds et al., 1992; Beckwith & Baird, 2001).

In Fig. 2 the volumetric strain is plotted as a function of the difference between the mean total stress and the pore fluid pressure, u_f, measured at the bottom of the sample. Three different behaviour stages can be identified. During stage 1, the response of the two samples almost coincided with a very small amount of gas generated ($\varepsilon_p \approx 0.01$). The production of gas increased up to $\varepsilon_p \approx 0.05$ - 0.06 over stage 2, at the expenses of a dramatic reduction in $p - u_f$. Eventually, significant gas expansion occurred during the final stage 3 under a very small and nearly constant confining stress $p - u_f \approx 3$ kPa.

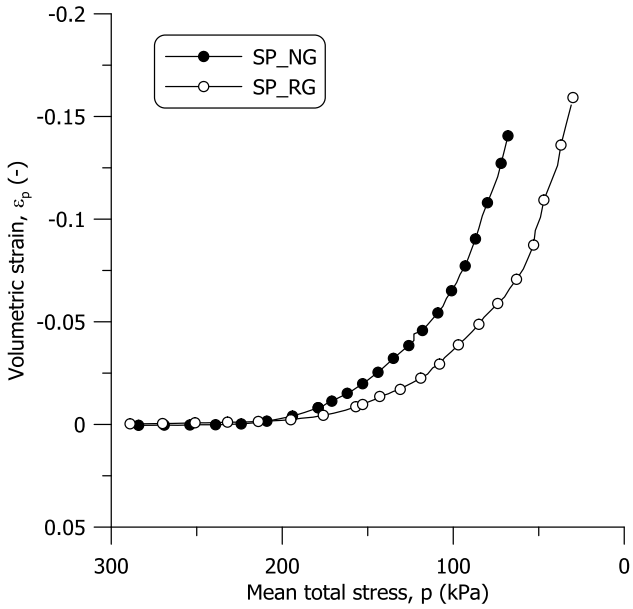

Fig. 1. Volumetric strain during isotropic undrained unloading of gassy peat samples

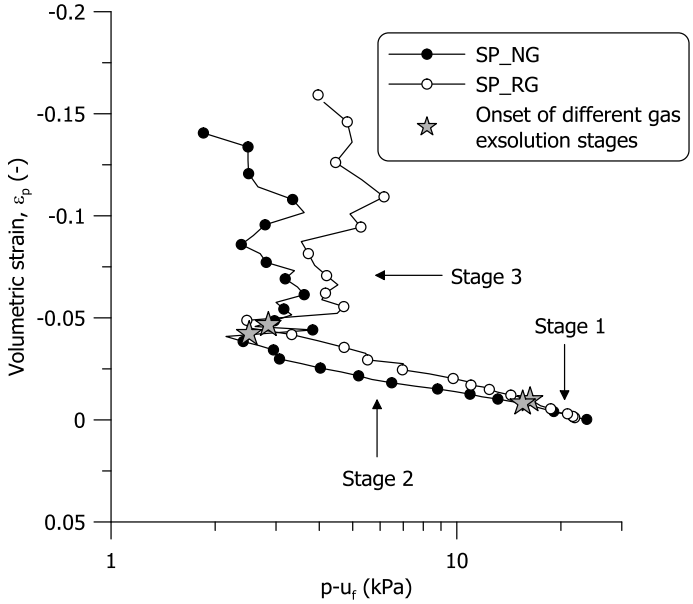

Fig. 2. Volumetric strain plotted against the difference between the mean total stress and the measured pore fluid pressure during isotropic undrained unloading

The observed mechanical response was preliminary discussed by Jommi et al. (2019), who suggested that different gas-liquid-solid interaction processes dominate the response depending on the different relative volume occupied by the gas bubbles within the porous space. During stage 1, the response is that of a porous medium saturated with a compressible pore fluid, due to entrapment of the gas bubbles in the liquid phase. Over stage 2, the gas bubbles start interacting with the soil

skeleton. The soil is able to sustain further gas pressure increase, until the difference between the total external stress and the measured pore pressure approaches zero, when the soil experiences an abrupt increase of its volume (stage 3).

Drying test

Experimental data from the drying and the shrinkage tests on samples SP_RD were combined to obtain a water retention curve linking the degree of saturation, S_r, to the gas - liquid pressure difference, $u_g - u_l$, over main drying. During the test, liquid pressure and water mass loss are measured. The current water content, w, can be expressed in terms of water ratio, $e_w = G_s w$, and the shrinkage curve, linking the water ratio to the void ratio, e, is used to evaluate the degree of saturation, $S_r = e_w/e$. The shrinkage curve and the estimated water retention curve are displayed in Fig. 3.

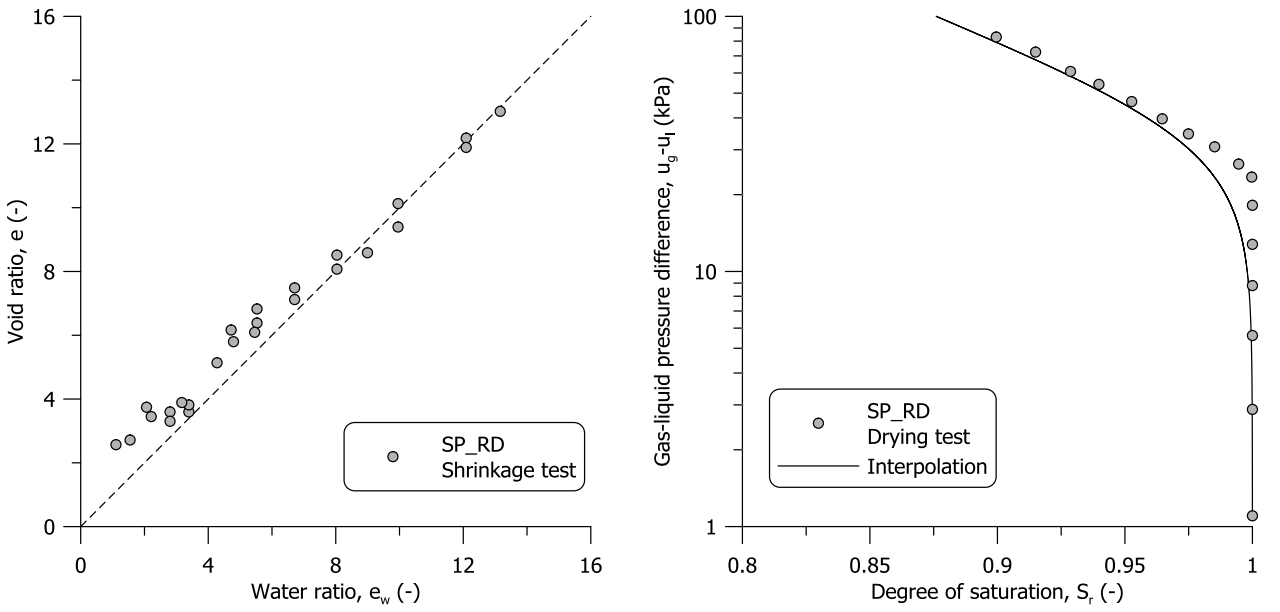

(a) (b)

Fig. 3. Results from drying: (a) shrinkage curve and (b) water retention curve

The data in Fig. 3(b) can be interpolated with a Van Genuchten's equation (3) with $\alpha = 0.028$ kPa^{-1}, $\beta = 0.05$ and $\gamma = 2.5$

$$u_g - u_l = \frac{1}{\alpha}\left[\left(S_r^{-\frac{1}{\beta}}\right) - 1\right]^{\frac{1}{\gamma}} \quad (1)$$

The results show that the peat sample can sustain relatively high difference between gas and liquid pressures without significant desaturation, if shrinkage is allowed. From Fig. 3(b), an air entry value (AEV) in the range 20 - 30 kPa can be inferred for the tested peat.

Comparing gas exsolution and drying

The degree of saturation of the samples undergoing undrained unloading was estimated from the volumetric strains obtained from the test data (i.e. $\delta S_r/S_r = -\delta e/e$ with $\delta e = -(1+e)\delta\varepsilon_p$). The corresponding values at the beginning of stage 2 ($S_r \approx 0.99$) and stage 3 ($S_r \approx 0.94$) are projected in Fig. 4 on the retention curve estimated from the drying tests (equation (1)). Over the first stage, the soil is semi-saturated and the small amount of exsolved gas bubbles remains isolated into the water phase. The start of stage 2 corresponds to the air entry value, $(u_g - u_l) \approx 20$ kPa, found for the same peat during the drying test. Stage 3 during unloading initiates when the degree of saturation reaches a value $S_r \approx 0.94$. The difference between the gas and the liquid pressures corresponding to this degree of saturation on the water retention curve is $(u_g - u_l) \approx 50$ kPa.

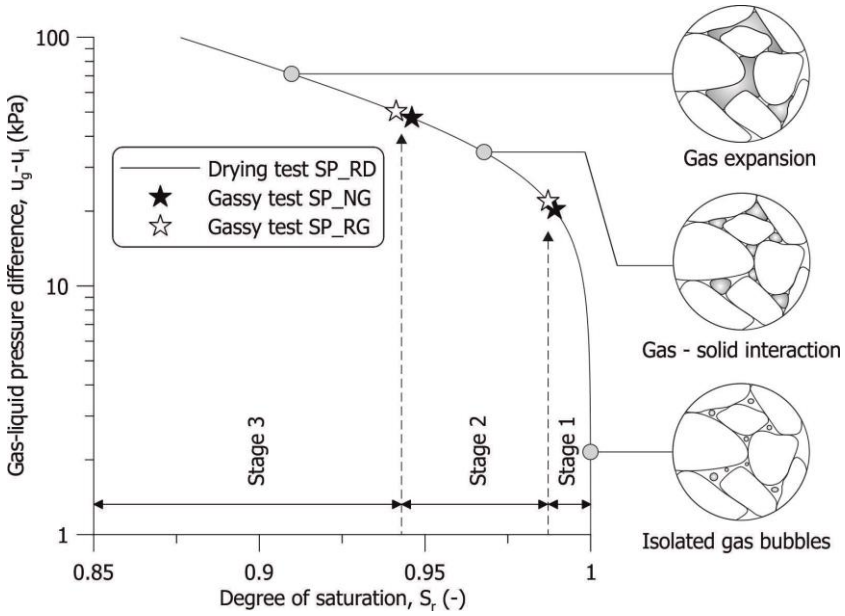

Fig. 4. Projection of the different gas exsolution stages on the retention curve

MODELLING

The development of a modelling approach primarily requires choosing convenient stress variables. The choice for gassy soils is complicated by the fact that the gas pressure can hardly be measured directly. The modelling framework is built on the hypothesis that the difference between the gas and the liquid pressure, s,

$$s = u_g - u_l \tag{2}$$

and the "average skeleton stress", $\hat{p}$, (Jommi, 2000)

$$\hat{p} = p - \hat{u}_f \tag{3}$$

where the "average fluid pressure" $\hat{u}_f$ is defined as

$$\hat{u}_f = u_l + (1 - S_r)\left(u_g - u_l\right) \tag{4}$$

can be used as stress variables to model the volumetric response of the unsaturated peat, whatever process is responsible for desaturation, either drying or gas exsolution in the initially saturated matrix. The water retention curve in equation (1) is adopted to describe the relationship between $(u_g - u_l)$ and the degree of saturation for both processes.

The void ratio of the soil is modelled by a unique function of the average skeleton stress and the gas - liquid pressure difference

$$e = f(\hat{p}, s) \tag{5}$$

Given the previous assumptions, also the water ratio, $e_w = S_r e$, turns out to be a unique function of the average skeleton stress and the gas - liquid pressure difference.

In the following, the compression behaviour of the soil is modelled with a common non-linear law, of the type

$$de = -\lambda(s)\,\frac{d\hat{p}}{\hat{p}} \tag{6a}$$

$$de = -\kappa(s)\,\frac{d\hat{p}}{\hat{p}} \tag{6b}$$

where $\lambda(s)$ is the slope of the virgin compression line (NCL), and $\kappa(s)$ is the slope of the unloading-reloading lines (URL). The compression indexes are allowed to vary with the gas –liquid pressure difference, to account for a huge body of experimental results indicating that the latter tends to modify the compressibility of unsaturated soils. When the soil is saturated, λ_{sat} and κ_{sat}

become the usual compression indexes, and can be obtained from standard saturated compression paths.

Simulations

The previous experimental data are exploited to verify whether the approach can encompass both desaturation processes. Some of the experimental information is used to simulate the tests, and the remaining measurements are compared to the model simulations. The value of λ_{sat} and κ_{sat} were chosen from the results of isotropic compression tests performed on saturated samples of the same peat (Muraro, 2019). Below the air entry value, the saturated compression index was used. In the absence of any direct information, λ and κ were tentatively reduced to 0.8 the saturated value above the air entry value to account for some reduction in the compressibility. In Table 2, the initial state of the samples and the parameters used in the simulations are summarised.

Table 2. Initial state and material parameters used in the simulations of undrained unloading

Sample ID	Type	$\hat{p}_0$ before unloading (kPa)	e_0 before unloading (-)	Slope of the saturated NCL, λ (-)	Slope of the saturated URL, κ (-)
SP_NG	Natural	24	8.7	--	0.18
SP_RG	Reconstituted	23	9.2	2.0	0.30

For the drying test, the simulation is driven by decreasing liquid pressure. The degree of water saturation is given by the water retention curve (equation (1)) and the change in void ratio is calculated with equation (6a). The simulation allows drawing the theoretical shrinkage curve and compare it with the measured data. The result reported in Fig. 5 shows that, in spite of the simplicity of the model, the shrinkage curve is nicely reproduced over the entire wide range of water ratio investigated.

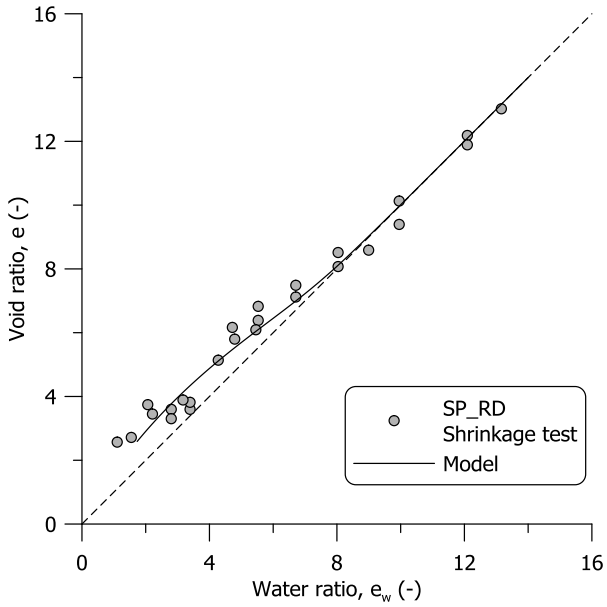

Fig. 5. Comparison between experimental results and model simulation of the shrinkage test

The simulation of the undrained unloading test is slightly more tricky, as the liquid phase had been artificially charged with dissolved gas before the start of the test. To describe the initial state, and to allow for gas exsolution at reducing external stress, Henry's law of solubility was added to the model. Henry's coefficient of solubility was set to 0.92, coming from the use of CO_2 in the experimental tests. Finite compressibility of the water, gas exsolution and gas expansion are accounted for, by integrating the relevant balance equations on a single element. The simulation is driven by the reduction of total mean stress at constant water mass (undrained unloading). The degree of water saturation is given by the water retention curve (equation (1)) and the change in void ratio is calculated with equation (6b). By solving the mass balance equations together with the constitutive equations, the volumetric strain, ε_p, and the fluid pressures, u_g and u_l can be independently calculated.

Fig. 6 shows the comparison between calculated and measured variables. In Fig. 6(a), the pressure measured at the bottom of the sample, u_f, is compared to the calculated average fluid pressure $\hat{u}_f$ (equation (4)), as a function of the controlling variable, p. The two coincide over the entire test, suggesting that the fluid pressure measured during the test can be reasonably identified with the average of the gas and liquid pressures weighted by their volume fraction, over the high saturation range investigated. Given this result, the degree of saturation and the volumetric strain are plotted as a function of the chosen constitutive stress in Fig. 6(b) and Fig. 6(c), respectively. The simulation results well match the experimental data until gas expansion dramatically softens the peat fabric. In this final stage, gas pockets developing at the boundaries of the samples were observed as a result of

preferential gas flow paths (Jommi et al., 2017). These localised phenomena, which are not included in the simple model presented in this study, are expected to be responsible for the difference between the experimental pressure threshold at which the peat softened and the results of the simulation.

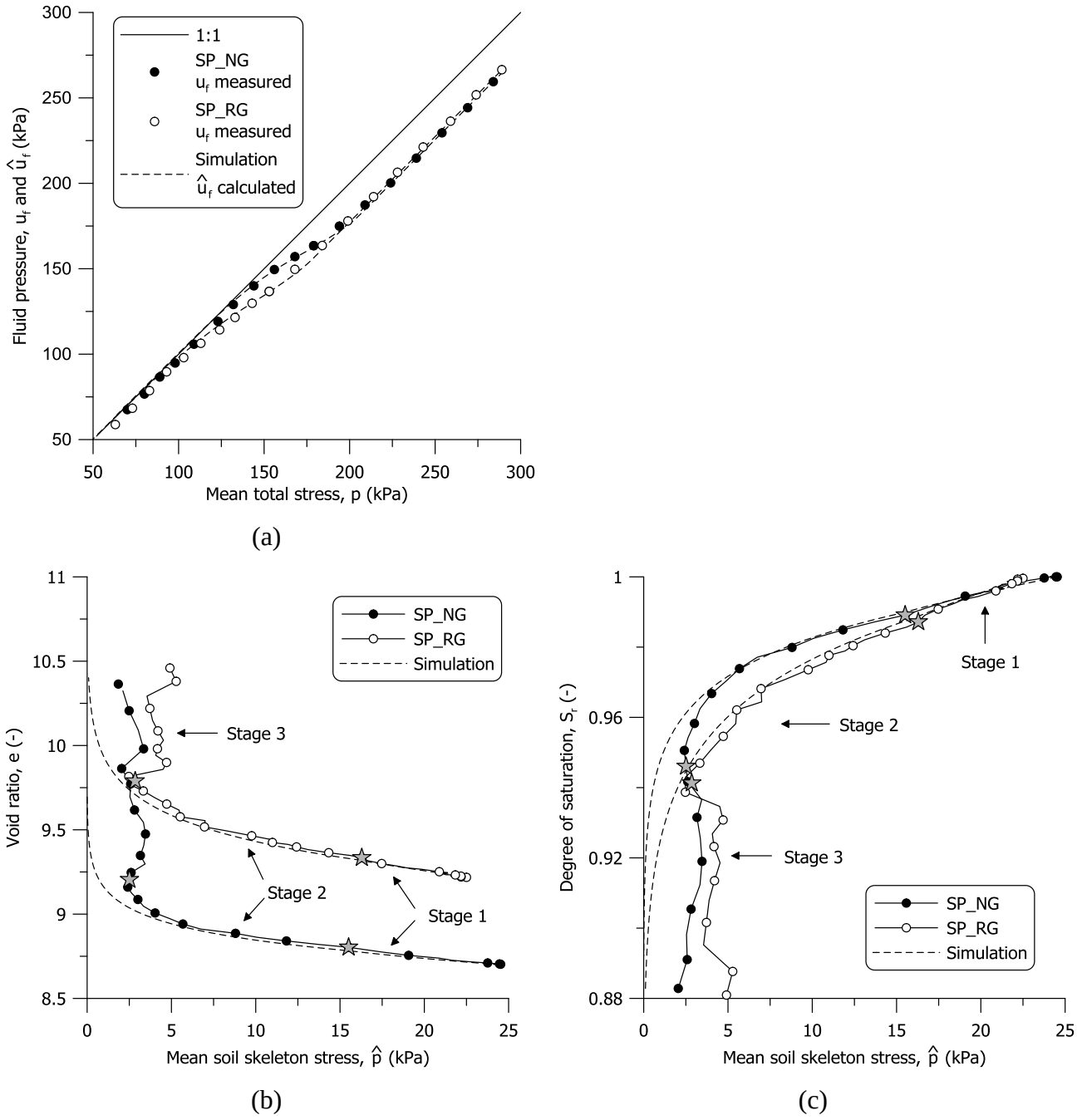

Fig. 6. Comparison between experimental results and model simulations: (a) measured and calculated pore fluid pressure, (b) void ratio and (c) degree of saturation

CONCLUSIONS

Experimental results from gassy peat samples were combined with drying tests to highlight analogies between gas exsolution and gas invasion. At the onset of gas exsolution, the gas bubbles remain confined in the liquid phase until, with further exsolution and expansion, gas bubbles start acting directly on the soil skeleton. The transition between these two stages seems to correspond to the air entry value on the retention curve derived from drying tests. Based on this result, a preliminary modelling approach derived from classical unsaturated soil mechanics has been adapted to reproduce the mean features of gas exsolution in peat. The model simulations were able to reproduce quite well the pore pressure development in gassy peats upon undrained unloading and the corresponding amount of gas exsolved for the imposed stress history. Although preliminary, the results of this work suggest that a comprehensive constitutive framework, relying on a unique gas-liquid pressure difference – liquid saturation relationship, can encompass both drying and gas exsolution in organic soils.

ACKNOWLEDGEMENTS

The financial contribution of the European Commission to this research through the Marie Curie Industry-Academia Partnership and Pathways Network MAGIC (Monitoring systems to Assess Geotechnical Infrastructure subjected to Climatic hazards) – PIAPP-GA-2012-324426 – is gratefully acknowledged. The first author thanks the financial contribution of the National Natural Science Foundation of China (No. 51909287) and Guangdong provincial Natural Science Foundation of China (No. 2020A1515010872).

REFERENCES

Acharya, M. P., Hendry, M. T. & Edwards, T. (2015). A Case Study of the Long-Term Deformation of Peat beneath an Embankment Structure. In From Fundamentals to Applications in Geotechnics: Proceedings of the 15th Pan-American Conference on Soil Mechanics and Geotechnical Engineering. IOS Press, Buenos Aires, Argentina, pp. 438-446.

Acharya, M. P., Hendry, M. T. & Martin, C. D. (2016). Thermally induced pore pressure response in peat beneath a railway embankment. International Journal of Geotechnical Engineering **10(2)**:145-154.

Ata-Ur-Rehman, T. & Durnford, D. S. (1993). Soil volumetric shrinkage measurements: a simple method. Soil Science **155(5)**:325-330.

Beckwith, C. W. & Baird, A. J. (2001). Effect of biogenic gas bubbles on water flow through poorly decomposed blanket peat. Water Resources Research **37(3)**:551-558.

D2974-14 (2014). Standard test methods for moisture, ash, and organic matter of peat and other organic soils. American Society of Testing and Materials.

Dai, S. & Santamarina, J. C. (2013). Water retention curve for hydrate-bearing sediments. Geophysical Research Letters **40(21)**:5637-5641.

den Haan, E. J. & Kruse, G. a. M. (2007). Characterisation and engineering properties of Dutch peats. In Proceedings of the Second International Workshop of Characterisation and Engineering Properties of Natural Soils. (Tan, Phoon, Hight, and Leroueil (eds.)) Taylor & Francis Group, Singapore, vol. 29, pp. 2101-2133.

Gebhardt, S., Fleige, H. & Horn, R. (2010). Shrinkage processes of a drained riparian peatland with subsidence morphology. Journal of soils and sediments **10(3)**:484-493.

Glaser, P. H., Chanton, J. P., Morin, P., Rosenberry, D. O., Siegel, D. I., Ruud, O., Chasar, L. I. & Reeve, A. S. (2004). Surface deformations as indicators of deep ebullition fluxes in a large northern peatland. *Global Biogeochemical Cycles* **18(1)**:1-15.

Grozic, J. L. H., Nadim, F. & Kvalstad, T. J. (2005). On the undrained shear strength of gassy clays. Computers and Geotechnics **32(7)**:483-490.

Hobbs, N. B. (1986). Mire morphology and the properties and behaviour of some British and foreign peats. Quarterly Journal of Engineering Geology and Hydrogeology **19(1)**:7-80.

Jang, J. & Santamarina, J. C. (2014). Evolution of gas saturation and relative permeability during gas production from hydrate-bearing sediments: Gas invasion vs. gas nucleation. Journal of Geophysical Research: Solid Earth **119(1)**:116-126.

Jommi, C. (2000). Remarks on the constitutive modelling of unsaturated soils. In Experimental evidence and theoretical approaches in unsaturated soils. (Tarantino and Mancuso (eds.)) Balkema: Rotterdam, pp. 139-153.

Jommi, C., Muraro, S., Trivellato, E. & Zwanenburg, C. (2017). Evidences of the Effects of Free Gas on the Hydro-mechanical Behaviour of Peat. In Advances in Laboratory Testing and Modelling of Soils and Shales. (Ferrari and Laloui (eds.)) Springer, Cham, Switzerland, pp. 112-119.

Jommi, C., Muraro, S., Trivellato, E. & Zwanenburg, C. (2019). Experimental results on the influence of gas on the mechanical response of peats. Géotechnique **69(9)**:753-766.

Kimoto, S., Oka, F., Fushita, T. & Fujiwaki, M. (2007). A chemo-thermo-mechanically coupled numerical simulation of the subsurface ground deformations due to methane hydrate dissociation. Computers and Geotechnics **34(4)**:216-228.

Landva, A. O. & Pheeney, P. E. (1980). Peat fabric and structure. Canadian Geotechnical Journal **17(3)**:416-435.

Minayeva, T. Y. & Sirin, A. A. (2012). Peatland biodiversity and climate change. Biology Bulletin Reviews **2(2)**:164-175.

Muraro, S. (2019). The deviatoric behaviour of peat: a route between past empiricism and future perspectives. PhD thesis. Delft University of Technology.

Page, S. E., Siegert, F., Rieley, J. O., Boehm, H.-D. V., Jaya, A. & Limin, S. (2002). The amount of carbon released from peat and forest fires in Indonesia during 1997. Nature **420(6911)**:61-65.

Peng, X., Horn, R. & Smucker, A. (2007). Pore shrinkage dependency of inorganic and organic soils on wetting and drying cycles. Soil science society of America journal **71(4)**:1095-1104.

Price, J. S. (2003). Role and character of seasonal peat soil deformation on the hydrology of undisturbed and cutover peatlands. Water Resources Research **39(9)**:1-10.

Reynolds, W. D., Brown, D. A., Mathur, S. P. & Overend, R. P. (1992). Effect of in-situ gas accumulation on the hydraulic conductivity of peat. Soil Science **153(5)**:397-408.

Sánchez, M., Santamarina, C., Teymouri, M. & Gai, X. (2018). Coupled Numerical Modeling of Gas Hydrate-Bearing Sediments: From Laboratory to Field-Scale Analyses. Journal of Geophysical Research: Solid Earth **123(12)**:10,326-10,348.

Sanchez, M. & Santamarina, J. C. (2010). Analysis of hydrate bearing sediments using a fully coupled THMC formulation. In Fifth International Conference on Unsaturated Soils, Barcelona, Spain, pp. 6-8.

Skempton, A. W. & Petley, D. J. (1970). Ignition loss and other properties of peats and clays from Avonmouth, King's Lynn and Cranberry Moss. Géotechnique **20(4)**:343-356.

Sultan, N. & Garziglia, S. (2014). Mechanical behaviour of gas-charged fine sediments: model formulation and calibration. Géotechnique **64(11)**:851-864.

Trivellato, E. (2014). The effects of partial saturation on the geotechnical properties of peats: an experimental investigation. MSc thesis. Politecnico di Milano.

Ums (2012). User Manual HYPROP, version 02.13. UMS GmbH, Munich.

Van Der Werf, G. R., Morton, D. C., Defries, R. S., Olivier, J. G. J., Kasibhatla, P. S., Jackson, R. B., Collatz, G. J. & Randerson, T. (2009). CO_2 emissions from forest loss. Nature geoscience **2(11)**:737-738.

Vonk, B. F., Den Haan, E., Termaat, R. & Edil, T. B. (1994). Some aspects of the engineering practice regarding peat in small polders. In Advances in understanding and modelling mechanical behaviour of peat. (Den Haan, Termaat, and Edil (eds.)) Balkema, pp. 389-402.

Wheeler, S. J. (1988). A conceptual model for soils containing large gas bubbles. Géotechnique **38(3)**:389-397.

Wösten, J. H. M., Ismail, A. B. & Van Wijk, A. L. M. (1997). Peat subsidence and its practical implications: a case study in Malaysia. Geoderma **78(1-2)**:25-36.

Yang, M. & Liu, K. (2016). Deformation behaviors of peat with influence of organic matter. SpringerPlus **5(1)**:573.

LIST OF SYMBOLS

S_r	degree of saturation of the liquid phase (-)
u_l	liquid pressure (kPa)
u_g	gas pressure (kPa)
u_f	measured fluid pressure (kPa)
s	gas - liquid pressure difference (kPa)
p	mean total stress (kPa)
$\hat{p}$	mean soil skeleton stress (kPa)
$d\hat{p}$	incremental mean soil skeleton stress change (kPa)
$\hat{u}_f$	calculated average fluid pressure (kPa)
ε_p	volumetric strain (-)
w	water content (-)
G_s	specific gravity (-)
e	void ratio (-)
e_w	water ratio (-)
de	incremental void ratio change (-)
$\hat{p}_0$	mean soil skeleton stress before unloading (kPa)
e_0	void ratio before unloading (-)
λ_{sat}	slope of virgin compression line for fully saturated soil (-)
κ_{sat}	slope of the unloading-reloading lines for fully saturated soil (-)
$\lambda(s)$	slope of virgin compression line function of the gas - liquid pressure difference (-)
$\kappa(s)$	slope of the unloading-reloading lines function of the gas - liquid pressure difference (-)
α	parameter of the retention curve (kPa^{-1})
β, γ	parameters of the retention curve (-)